无 机 化 学 学 报

2020年　　第36卷　　第8期

目　次

论　文

CHINESE JOURNAL OF INORGANIC CHEMISTRY

Vol.36 No.8 Aug. 2020

CONTENTS

Cover

Articles

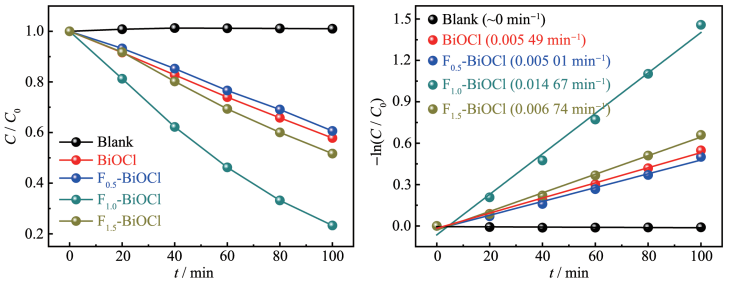

Novel F-doped BiOCl photocatalyst with exposed (001) facets was prepared by a facile solvothermal-calcination route. Fluorine doping effectively improved the separation efficiency of photogenerated carriers, and the fabricated F-BiOCl displayed excellent performance in the removal of dye pollutants.

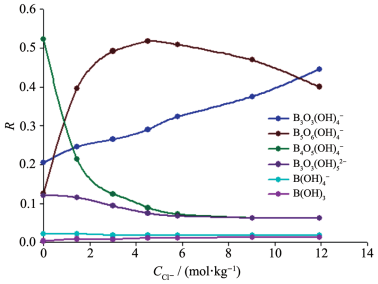

$MgCl_2$ concentration has a great influence on $Mg(BO_2)_2$ dissociated in aqueous $MgCl_2$ solution. With the increasing of $MgCl_2$, the solid species changed gradually from $Mg_2B_6O_{11}\cdot 15H_2O$ and $Mg(OH)_2$ to $Mg_2B_6O_{11}\cdot 15H_2O$ and $Mg_3Cl_2(OH)_4\cdot 4H_2O$, and main species of polylobate anions in liquid phase changed gradually from $B_4O_5(OH)_4^{2-}$ and $B_3O_3(OH)_4^-$ to $B_3O_3(OH)_4^-$ and $B_5O_6OH)_4^-$.

Helical Coordination Polymers Based on Tetra-coordinated Co(Ⅱ): Syntheses, Structures and Photocatalytic CO_2 Reduction Reaction

XU Zhong-Xuan, LI Li-Feng, BAI Xu-Ling

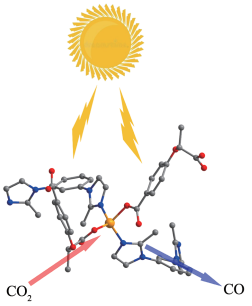

Helical homochiral coordination polymers based on lactic acid derivatives and tetra-coordinated Co(Ⅱ) centers were synthesized and used as photocatalysts for CO_2 reduction reaction.

DOI:10.11862/CJIC.2020.154
Chinese J. Inorg. Chem., **2020**,**36**(8):1430-1436

Effects of Astragalus Polysaccharides with Different Molecular Weights on Calcium Oxalate Crystal Growth and Cytotoxicity

CHEN Xue-Wu, HUANG Fang, OUYANG Jian-Ming

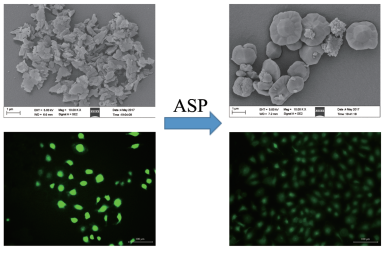

Four different molecular weight ASPs are not only non-toxic, but also have the ability to inhibit COM growth, induce COD production and repair damaged HK-2 cells. This ability is closely related to their own molecular weight.

DOI:10.11862/CJIC.2020.164
Chinese J. Inorg. Chem., **2020**,**36**(8):1437-1445

One-Step Preparation and Photocatalytic Activity of $Bi_2MoO_6/CoMoO_4$ Embroidery Ball Structure

ZHANG Zhi, ZOU Chen-Tao, YANG Zhi-Yuan, YANG Shui-Jin

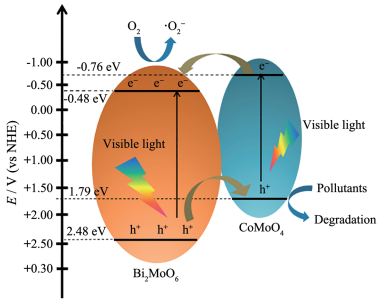

$Bi_2MoO_6/CoMoO_4$ heterojunction was obtained by facile synthesis method and showed excellent visible-light-driven towards the degradation of methylene blue and ceftriaxone sodium.

DOI:10.11862/CJIC.2020.162
Chinese J. Inorg. Chem., **2020**,**36**(8):1446-1456

Multi-scale Ag/CuO Photothermal Materials: Preparation and Application in Seawater Desalination

LI Zheng-Tong, WANG Cheng-Bing

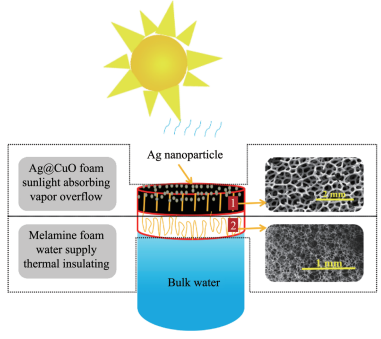

Multi-scale Ag/CuO composites were prepared by *in-situ* chemical reaction, heat treatment and evaporative deposition technology and applied to interfacial photothermal desalination successfully. The effects of light trap structure design and novel metal doping on the properties of metal-based composite photothermal materials were explored.

DOI:10.11862/CJIC.2020.160
Chinese J. Inorg. Chem., **2020**,**36**(8):1457-1464

Effect of Surfactant on Structure and Properties of $LiNi_{0.80}Co_{0.15}Al_{0.05}O_2$

HUANG Ling, WANG Ying, TANG Ren-Heng, XIAO Fang-Ming, LI Wen-Chao

DOI:10.11862/CJIC.2020.111
Chinese J. Inorg. Chem., **2020**,**36**(8):1465-1474

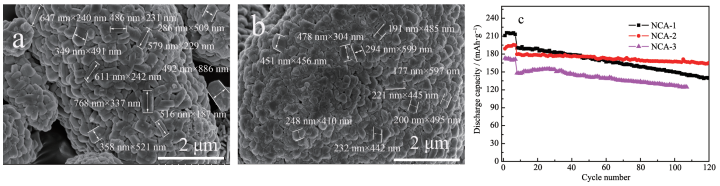

With the addition of PVP and PEG, the growth of primary grains is improved, resulting in the excellent electrochemical performance of NCA which displayed a high discharge capacity of 210.8 and 188.9 $mAh\cdot g^{-1}$, and showed good capacity retention of 78.8% and 93.2% after 100 cycles.

Heteropoly Acid Grafted-MOFs Functionalized Magnetic Composite Material for Catalytic Oxidative Desulfurization

ZHANG Han, WANG Jun-Er, DONG Hao, YANG Ni-Ni, PAN Lin-Yun, SHEN Hao-Yu, HU Mei-Qin, CHENG Jin-Jin

DOI:10.11862/CJIC.2020.153
Chinese J. Inorg. Chem., **2020**,**36**(8):1475-1484

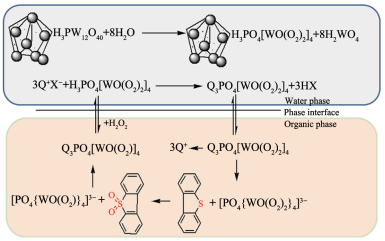

Heteropoly acid grafted-MOFs functionalized magnetic composite material HPW@Fe_3O_4-COOH@MIL-101(Cr) was prepared and showed good catalytic desulfurization performance with reusability.

Effects of Rare Earths (Gd^{3+}, La^{3+}) on Fluorescence and Temperature Sensitivity of Eu(*p*-MOBA)$_3$phen/PMMA

TANG Juan, SUN Jing, ZHOU Chen, ZHAO Ying, GUO Xin, YIN Yu-Ting

DOI:10.11862/CJIC.2020.145
Chinese J. Inorg. Chem., **2020**,**36**(8):1485-1491

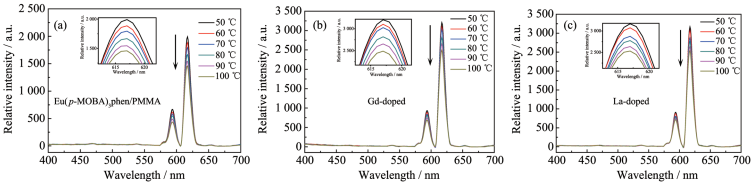

Rare earth ions (Gd^{3+}, La^{3+}) have a gain effect on the luminescence of Eu(*p*-MOBA)$_3$phen, and the corresponding TSPs have good fluorescence temperature quenching property in the temperature range of 50~100 ℃.

Tungsten Doped Iron-Nickel Layered Hydroxide for Oxygen Evolution and Hydrogen Evolution Reaction

LI Chun, TIAN Peng, PANG Hong-Chang, YE Jun-Wei, NING Gui-Ling

DOI:10.11862/CJIC.2020.163
Chinese J. Inorg. Chem., **2020**,**36**(8):1492-1498

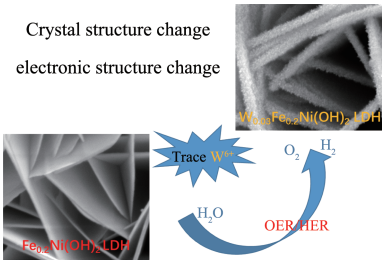

Ttrace W^{6+} ions doping can modulate $Fe_{0.2}Ni(OH)_2$ LDH crystal structure and enhance block electrons interaction, showing the low overpotential in the OER and HER.

Preparation and Photocatalytic Properties of Ag/Bi_2WO_6 Composites

LIU Yong, ZAN Jia-Hui, CHEN Ying, FAN Qu-Li

DOI:10.11862/CJIC.2020.144
Chinese J. Inorg. Chem., **2020**,**36**(8):1499-1505

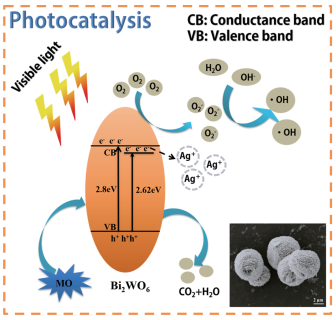

Spherical Ag/Bi_2WO_6 photocatalysts were prepared by hydrothermal synthesis. Due to the doping of Ag, the band gap of Bi_2WO_4 is reduced and its photocatalytic performance is improved greatly.

Preparation of High Performance Tin Oxide Anode with Cobalt-Rich Porous Carbon

ZOU Jing-Yi, SUN Xiao-Gang, LI Rui, HE Qiang

DOI:10.11862/CJIC.2020.166
Chinese J. Inorg. Chem., **2020**,**36**(8):1506-1514

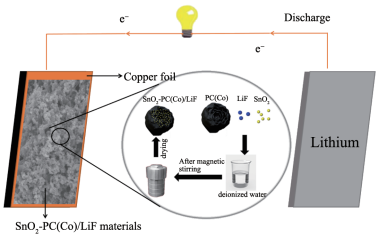

The porous carbon (PC(Co)) scaffold was used to host SnO_2 as a collector. Among them, the cobalt oxide in the PC(Co) material can enhance the electrochemical kinetics, but consume a certain amount of lithium ions. In order to ensure the superiority of batteries performance, LiF was added as a supplement to the lithium source.

Preparation and Electrochemical Performance of $Li_{6.4}La_3Zr_{1.4}Ta_{0.6}O_{12}$/Polymer-Based Solid Composite Electrolyte

TU Fang-Fang, XIE Jian, GUO Feng, ZHAO Xin-Bing, WANG Yu-Ping, CHEN Dong, XIANG Jia-Yuan, CHEN Jian

DOI:10.11862/CJIC.2020.169
Chinese J. Inorg. Chem., **2020**,**36**(8):1515-1523

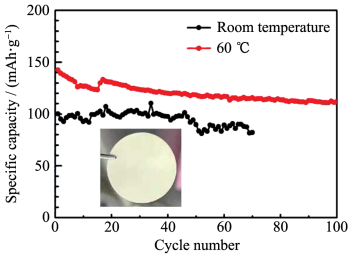

A solid composite electrolyte possesses a high ionic conductivity of 1.14×10^{-4} S·cm^{-1}. The $LiFePO_4$/Li cell with solid electrolyte exhibits a discharge capacity of 100.1 mAh·g^{-1} and a high capacity retention rate of 82% after 70 cycles at 0.1C.

Facile Synthesis and Sodium Storage Performance of N,Se-Co-doped Carbon Restricted NiSe Nanocrystalline Through a Two Step Direct Solid State Reaction

WANG Zhuang-Zhuang, LIU Sang-Xin, HOU Qi-Rui, ZHANG Li-Cui, ZHANG An-Ping, WU Ping, ZHU Xiao-Shu, WEI Shao-Hua, ZHOU Yi-Ming

DOI:10.11862/CJIC.2020.167
Chinese J. Inorg. Chem., **2020**,**36**(8):1524-1534

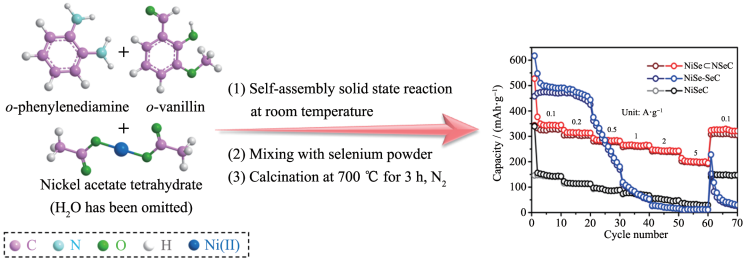

NiSe nanocrystallines confined within a N,Se-codoped carbon scaffold are readily *in-situ* fabricated via a two step direct solid state reaction, which demonstrate exceptional electrochemical performances as anode materials for sodium-ion batteries.

Preparation and Photocatalytic Hydrogen Production of Bi/Yb^{3+}, Er^{3+}:TiO_2 Nanofibers

ZHAO Xiao-Bo, LI Yue-Jun, CAO Tie-Ping, SUN Da-Wei

DOI:10.11862/CJIC.2020.174
Chinese J. Inorg. Chem., **2020**,**36**(8):1535-1542

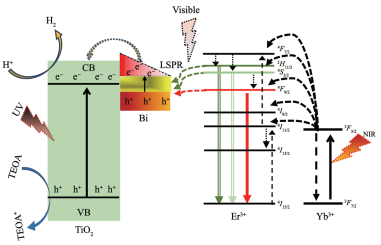

The Bi/Yb^{3+}, Er^{3+}:TiO_2 composite naofibers were prepared by locating the Bi naoparticles through hydrothermal synthesis on the electrospun TiO_2 in the presence of NaH_2PO_2, which suggested that the photocatalysts got well photocatalytic activity and stability.

Electrochemical Preparation of MoS_2 Intercalated Compound with Micron Size for Magnesium-Ion Storage

LI Jin-Jin, LIU Cong-Cong, GUO Min, LI Shi-Ying, WU Zi-Chen, ZHAO Xiao-Li, YANG Xiao-Wei

DOI:10.11862/CJIC.2020.173
Chinese J. Inorg. Chem., **2020**,**36**(8):1543-1549

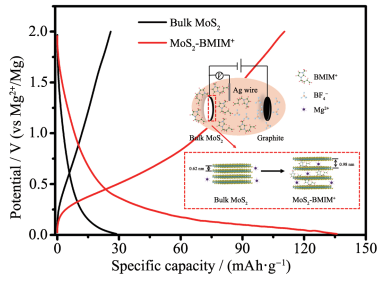

The micro-sized MoS_2 intercalated compound was prepared by a simple electrochemical method and used as cathode material of magnesium ion batteries. The MoS_2-$BMIM^+$ showed a significantly improved specific capacity (101.93 mAh·g^{-1} at 20 mA·g^{-1}, about 4 times as much as bulk MoS_2).

Three Complexes Constructed Using 2,2′-Oxybis(benzoic acid) and N-Donor Ligands: Syntheses, Structures and Fluorescent Properties (English)

TANG Long, FU Yu-Hao, WANG Yi-Tong, WANG Huan-Huan, WANG Ji-Jiang, HOU Xiang-Yang, WANG Xiao

DOI:10.11862/CJIC.2020.180
Chinese J. Inorg. Chem., **2020**,**36**(8):1550-1556

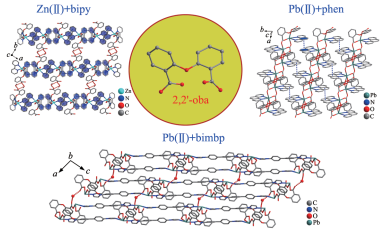

The 2,2′-oxybis(benzoic acid) was employed in transitional metal Zn(Ⅱ)/Pb(Ⅱ) salts/chelate ligand/linear ligand systems to generate one 0D structure and two 1D chains. Moreover, the solid-state fluorescent properties of **1**~**3** have also been investigated. According to the crystal structures, the TDDFT/6-31G(d) approach was applied to study the photoluminescence emission of complex **1**.

CDs-Induced Polymorphous $CaCO_3$ Mineralization and Formation Mechanism (English)

ZHANG Da-Qin, JIA Zhi-Gang, LUO Guang-Cheng, WANG Hong-Zhou, LI Chao-Yong, WU Lin, CHEN Qi-Hou

DOI:10.11862/CJIC.2020.179
Chinese J. Inorg. Chem., **2020**,**36**(8):1557-1566

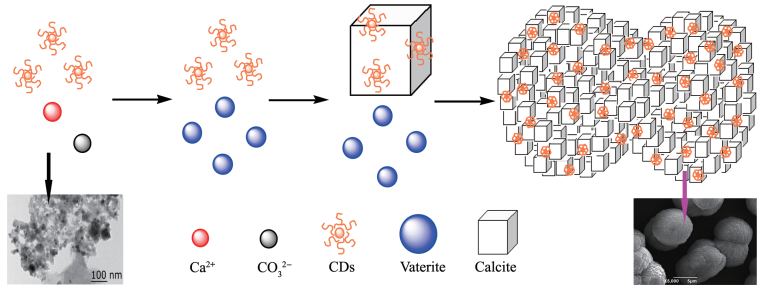

Pentanuclear Sn(Ⅱ) Guanidinate Complex: Synthesis, Structure, and Catalytic Activity for Addition of Arylamines into *N*,*N*′-Diisopropylcarbodiimide (English)

WANG Ying-Ying, TONG Hong-Bo, ZHOU Mei-Su

DOI:10.11862/CJIC.2020.178
Chinese J. Inorg. Chem., **2020**,**36**(8):1567-1572

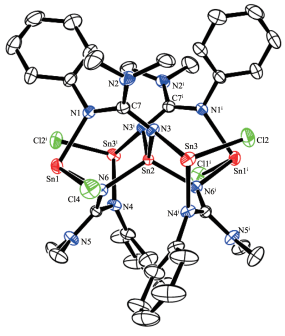

A pentanuclear Sn(Ⅱ) complex stabilized by guanidinate ligands is presented. It is an active catalyst in the addition reaction of arylamines to *N*,*N*′-diisopropylcarbodiimide.

Preparation and Application in Supercapacitors of Shiitake Biomass-Based Nitrogen-Doped Microporous Carbon (English)

HU Qing-Tao, ZHANG Wen-Da, LI Tao, YAN Xiao-Dong, GU Zhi-Guo

DOI:10.11862/CJIC.2020.114
Chinese J. Inorg. Chem., **2020**,**36**(8):1573-1581

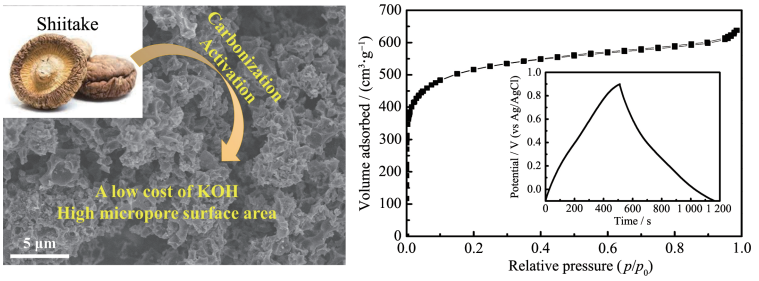

Shiitake-derived nitrogen-rich microporous carbons presented a high micropore surface area of 1 594 $m^2 \cdot g^{-1}$, a high capacitance of 325 $F \cdot g^{-1}$ at 0.5 $A \cdot g^{-1}$, good rate capability, and robust stability.

Construction of MoS_2/Tubular-like g-C_3N_4 Composite Photocatalyst for Improved Visible-Light Photocatalytic Hydrogen Production from Seawater (English)

SHI Wei-Long, YANG Shuang, WANG Jing-Bo, LIN Xue, GUO Feng, SHI Jun-You

DOI:10.11862/CJIC.2020.168
Chinese J. Inorg. Chem., **2020**,**36**(8):1582-1592

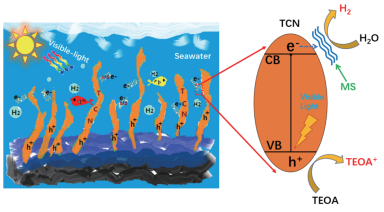

2D/1D heterostructure MoS_2/tubular g-C_3N_4 nanocomposite photocatalyst showed outstanding visible-light photocatalytic activity hydrogen production from seawater.

Morphology-Controlled Syntheses and Functionalization of Trivacant Silicotungstate Nano-materials (English)

LIU Ning, WANG Jia-Xin, WU Ya-Ning, CHEN Yu-Hao, WANG Guan, ZHANG Dong-Di

DOI:10.11862/CJIC.2020.175
Chinese J. Inorg. Chem., **2020**,**36**(8):1593-1604

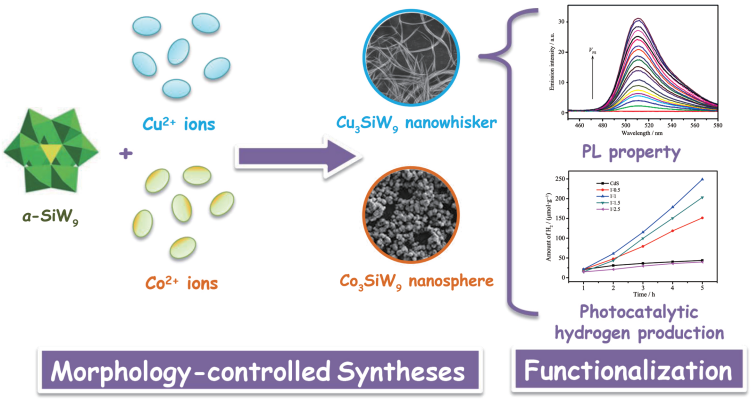

Transition metal ions were used as dopant to control the morphologies of silicotungstate nano-materials successfully. Moreover, the properties of derivative nanocomposites FS-Cu_3SiW_9 and CdS/Cu_3SiW_9 were also studied.

Growth Process, Photoluminescence Property and Photocatalytic Activity of SnO_2 Nanorods (English)

ZHAN Hong-Quan, DENG Ce, LIU Quan, LI Xiao-Hong, XIE Zhi-Peng, WANG Chang-An

DOI:10.11862/CJIC.2020.176
Chinese J. Inorg. Chem., **2020**,**36**(8):1605-1612

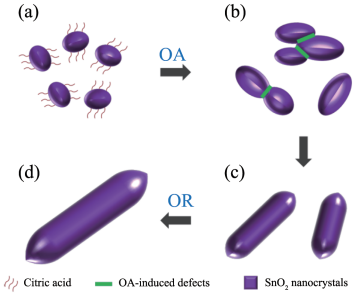

SnO_2 nanorods growth follows "Oriented Attachment+Ostwald Ripening" and the concentration of OA-induced defects result in different property.